IOP PUBLISHING JOURNAL OF PHYSICS A: MATHEMATICAL AND THEORETICAL

J. Phys. A: Math. Theor. **41** (2008) 115202 (15pp) doi:10.1088/1751-8113/41/11/115202

Explicit near-symplectic mappings of Hamiltonian systems with Lie-generating functions

Y Kominis[1], K Hizanidis[1], D Constantinescu[2] and O Dumbrajs[3,4]

[1] School of Electrical and Computer Engineering, National Technical University of Athens, Association EURATOM–Hellenic Republic, Zographou GR-15773, Greece
[2] Department of Applied Mathematics, University of Craiova, A I Cuza Street 13, Craiova 1100, 200585 Romania
[3] Department of Engineering Physics and Mathematics, Helsinki University of Technology, Association EURATOM–TEKES, FIN-02150 Espoo, Finland
[4] Institute of Solid State Physics, Association Euratom–University of Latvia, Kengaraga Street 8, LV-1063, Riga, Latvia

Received 20 November 2007, in final form 15 January 2008
Published 4 March 2008
Online at stacks.iop.org/JPhysA/41/115202

Abstract

The construction of explicit near-symplectic mappings for generic Hamiltonian systems with the utilization of Lie transforms is presented. The method is mathematically rigorous and systematically extended to high order with respect to a perturbation parameter. The explicit mappings are compared to their implicit counterparts, which use mixed-variable generating functions, in terms of conservation of invariant quantities, calculation speed and accurate construction of Poincaré surfaces of sections. The comparative study considers a wide range of parameters and initial conditions for which different time scales are involved due to large differences between internal and external frequencies of the system.

PACS numbers: 05.45.Ac, 05.45.Pq, 05.60.Cd, 52.20.Dq, 52.25.Fi

(Some figures in this article are in colour only in the electronic version)

1. Introduction

Mappings constitute a powerful method for studying dynamical systems from both the analytical and the numerical point of view [1]. Poincaré maps on a surface of section of the phase space have been used in order to study the phase-space topology of dynamical systems by reducing the dynamics of a continuous system to a discrete one of lower dimensionality. As an application of major importance we can refer to the fundamental problem of the stability of periodic orbits in Hamiltonian systems; utilization of Poincaré maps reduces this problem to the study of stability of fixed points for the corresponding mappings [2]. Among all the dynamical models occurring in physics and other applications, the class of Hamiltonian

systems is of significant importance, since whenever the dissipation is negligible, most of the fundamental models are within this class, while on the microscopic scale most of the physical systems are Hamiltonian by definition. Hamiltonian systems have the characteristic property of conserving certain invariant quantities defined in the phase space. This property characterizes the phase space of such systems as symplectic [3, 4].

Among the Hamiltonian systems of physical interest we can refer to the study of magnetic-field lines in magnetically confined fusion plasmas in toroidal sytems such as tokamaks [5–11], the study of the magnetic structure in special devices of magnetic confinement such as ergodic and poloidal divertors [12, 13] and charged particle motion under the interaction with an electromagnetic wave [2, 14–16]. In other areas of physics, Hamiltonian models occur in the study of wave propagation, optics, accelerator physics and dynamical astronomy [2, 17–21].

From the point of view of numerical integration, standard methods are not ideal for solving Hamiltonian systems, since the respective approximations of the integration schemes introduce artificial non-Hamiltonian perturbations, and change completely the long-time behavior of the solutions, which appear as being effectively dissipative so that the conservation of the invariants of the motion is violated. In order to overcome these problems, a class of numerical integrators, known as symplectic integrators, has been constructed, so that the symplectic properties of a Hamiltonian system are preserved. This is assured by defining each integration step as a canonical (or symplectic) transformation.

Several approaches have been adopted for the construction of symplectic mappings. Among them we can refer to the method of *a priori* assumption of the symplectic form of the mapping resulting in the well-known perturbed twist mappings [2], and the method of the periodic delta functions, where a time-periodic perturbation acting on an integrable system is replaced by periodic delta functions, which has been used for the derivation of the standard map [22]. However, these methods are more or less heuristic and in lack of a sufficient mathematical justification. A mathematically rigorous method for the derivation of symplectic mappings has been developed by Abdullaev [23, 20] on the basis of the Hamilton–Jacobi theory and the canonical perturbation theory, which applies for generic Hamiltonian systems. However, all the aforementioned methods are implicit, namely the transformation equations defining each integration step involve implicit algebraic equations which have to be solved numerically with respect to the specific variables. The implicit form of the integration schemes results in a significant increasing of the time (CPU time) required for each step due to the iterative procedure (e.g. Newton–Raphson) which is used for the solution of the corresponding algebraic equations. On the other hand, explicit symplectic integrators have been provided only for the special class of separable systems in the form $H(q, p) = T(p) + V(q)$, where (q, p) are the canonical phase-space variables [24–26]. However, several models of important interest do not fall in this special class.

In this work, we present a method for constructing explicit near-symplectic mappings for Hamiltonian systems and study their performance in comparison with the implicit mappings. The canonical perturbation theory in finite time intervals with the utilization of Lie transforms [27, 28, 30] is used for providing the transformations defining the mapping governing the evolution of the canonical phase-space variables. Due to the truncation of the corresponding series expansions, the mappings are not exactly symplectic, but converge to the exactly symplectic mappings when the perturbation strength and/or the time step converge to zero. However, the explicit form of the mappings results in very fast calculations (in terms of CPU time) for each iteration step. The two mappings are compared in terms of accuracy and calculation speed for a wide range of parameters. Of particular interest is the case where very different frequencies are involved in the dynamics of the system such as differences between an internal frequency of a specific degree of freedom and an external frequency

of a driving (time-dependent) term of the Hamiltonian. The latter is considered as one of the challenging problems in numerical analysis (p 81 [20]). By comparing implicit and explicit maps of different orders we conclude that an implicit map, although more accurate, is also always more time-consuming than an explicit map of the same order, due to internal iterations required for solving the implicit algebraic equations in each step. However, we show that for quite small perturbations, which sometimes are met in physical applications, even a first-order explicit map can result in satisfactory accuracy. More importantly, we show that the calculation speed of explcit maps allows for the utilization of smaller time steps without increasing significantly the calculation (cpu) time. The latter results in advantageous performance of explicit maps in comparison to the implicit ones, since a better accuracy can be provided in the same computation time. Therefore, second-order explicit maps provide an alternative to implicit-maps solution which is useful for applications where high-speed, high-accuracy orbit calculations are needed.

The rest of this work is organized as follows: in section 2, the Lie-transform perturbation theory in finite time intervals is described briefly; in section 3, we consider a specific Hamiltonian system and compare the accuracy and calculation speed of implicit and explicit maps; finally, the main conclusions are summarized in section 4.

2. Lie-transform perturbation theory in finite time intervals

In this section we briefly summarize the basic concepts and results of Lie perturbation theory [27–29] as applied for finite time intervals. Although the method of Lie transforms is equivalent to the Poincaré–Von Zeipel method [30], there are at least two important advantages, in favor of this method: (i) the transformations as expressed in terms of Lie operators are significantly simpler, so that applying perturbation theory to higher order is practically possible only with Lie transforms, since the expressions involved in the Poincaré–Von Zeipel method become extremely complicated beyond second order, and (ii) all transformations are given explicitly in contrast to the Poincaré–Von Zeipel method which utilizes mixed-variable generating functions resulting in implicit expressions. Although, the latter comes with the cost of losing the exact symplectic property of the mapping, it leads to faster calculations, so that the overall performance of these explicit mappings has several advantages in comparison with their implicit counterparts, as we show in the next section.

In the following, we consider a general near-integrable system of the form

$$H(\mathbf{J},\theta,t) = H_0(\mathbf{J}) + \epsilon \sum_{m\neq 0} H_{\mathbf{m}}(\mathbf{J},t)\, \mathrm{e}^{\mathrm{i}\mathbf{m}\cdot\theta} \tag{1}$$

where $\mathbf{J} = (J_1,\ldots,J_N), \theta = (\theta_1,\ldots,\theta_N)$ are the action-angle variables of the unperturbed system H_0 and $\mathbf{m} = (m_1,\ldots,m_N), \mathbf{m}\cdot\theta = m_1\theta_1 + \cdots + m_N\theta_N$. The evolution of the phase-space variables $\mathbf{z} = (\mathbf{J},\theta)$ from time t_k to time t_{k+1} can be provided by the time-development operator $S_H(t_{k+1},t_k)$:

$$\mathbf{z}(t_{k+1}) = S_H(t_{k+1},t_k)\mathbf{z}(t_k) \tag{2}$$

The derivation of the operator $S_H(t_{k+1},t_k)$ is equivalent to solving the equations of motion, which is not possible for most of the cases. Instead, a change of variables in the transform

$$\mathbf{z}' = T(z,t)\mathbf{z} \tag{3}$$

can lead to a new system with Hamiltonian $K(\mathbf{z}',t)$, in which the time-development operator $S_K(t_{k+1},t_k)$ can easily be computed. These are the cases for which the new system is either integrable with $\mathbf{z}'$ corresponding to the action-angle variables the new Hamiltonian, or more

generally, when the new Hamiltonian does not depend on the phases and the action of the operator $S_K(t_{k+1}, t_k)$ leaves the actions unchanged and evolves the phases according to:

$$\mathbf{J}'(t_{k+1}) = \mathbf{J}'(t_k) \tag{4}$$

$$\theta'(t_{k+1}) = \theta'(t_k) + \int_{t_k}^{t_{k+1}} \omega_{\mathbf{K}}(J', s)\,\mathrm{d}s \tag{5}$$

where $\omega_{\mathbf{K}}(\mathbf{J}', t) = \partial K(\mathbf{J}', t)/\partial \mathbf{J}'$. In that sense, the solution of the system (1) can be obtained if the appropriate transformation T is constructed. According to the Lie transform theory, the operator T can be represented as

$$T = \mathrm{e}^{-L} \tag{6}$$

where $Lf = [w, f]$, for any function $f(\mathbf{z}, t)$, with $[\cdot, \cdot]$ denoting the Poisson bracket. The function $w(\mathbf{z})$ is defined as the Lie generator and the operator of the inverse transformation is $T^{-1} = \mathrm{e}^{L}$. Therefore, the evolution of the system can be calculated by subsequently transforming to a new variable set $\mathbf{z}'$, applying the time-development operator S_K and transforming back to the original variables $\mathbf{z}$, according to

$$\mathbf{z}(t_{k+1}) = T^{-1} S_K(t_{k+1}, t_k) T \mathbf{z}(t_k). \tag{7}$$

The aforementioned procedure, apart from being applicable to integrable system, also provides a perturbation method for solving approximately near-integrable systems, in which the Hamiltonian has a small nonintegrable part of order ϵ. In such cases the canonical transform T can be constructed as a power series in ϵ, by utilizing the method of Deprit [28], according to which the old Hamiltonian H, the new Hamiltonian K and the transformation T along with the Lie generator w are expanded in power series of ϵ:

$$H(\mathbf{z}, t, \epsilon) = \sum_{n=0}^{\infty} \epsilon^n H_n(\mathbf{z}, t) \tag{8a}$$

$$K(\mathbf{z}, t, \epsilon) = \sum_{n=0}^{\infty} \epsilon^n K_n(\mathbf{z}, t) \tag{8b}$$

$$T(\mathbf{z}, t, \epsilon) = \sum_{n=0}^{\infty} \epsilon^n T_n(\mathbf{z}, t) \tag{8c}$$

$$w(\mathbf{z}, t, \epsilon) = \sum_{n=0}^{\infty} \epsilon^n w_{n+1}(\mathbf{z}, t) \tag{8d}$$

where the expansion of w has been chosen appropriately in order to generate the identity transformation $T_0 = I$ to the lowest order. The transformations T and T^{-1} which will be used in the following are given below, through second order:

$$T_0 = I \tag{9a}$$

$$T_1 = -L_1 \tag{9b}$$

$$T_2 = -\tfrac{1}{2} L_2 + \tfrac{1}{2} L_1^2 \tag{9c}$$

$$T_0^{-1} = I \tag{10a}$$

$$T_1^{-1} = L_1 \tag{10b}$$

$$T_2^{-1} = \tfrac{1}{2} L_2 + \tfrac{1}{2} L_1^2 \tag{10c}$$

where $L_i f = [w_i, f]$. The equations providing the Lie generator w and the new Hamiltonian K to second order are:

$$K_0 = H_0 \tag{11}$$

$$\frac{\partial w_1}{\partial t} + [w_1, H_0] = K_1 - \sum_{\mathbf{m}\neq 0} H_{\mathbf{m}}(\mathbf{J}, t)\, \mathrm{e}^{\mathrm{i}\mathbf{m}\cdot\theta} \tag{12}$$

$$\frac{\partial w_2}{\partial t} + [w_2, H_0] = 2K_2 - L_1 K_1 - L_1 \left(\sum_{\mathbf{m}\neq 0} H_{\mathbf{m}}(\mathbf{J}, t)\, \mathrm{e}^{\mathrm{i}\mathbf{m}\cdot\theta} \right) \tag{13}$$

with the functions K_n being chosen arbitrarily. For an application of Lie transform perturbation theory to infinite time intervals, it is necessary to select the functions K_n so that the θ-independent part of the rhs is eliminated, in order to avoid secular terms. In this case the new Hamiltonian K is independent of θ. When finite time intervals are considered, the functions K_n can be alternatively set equal to zero, resulting in a zero Hamiltonian K and a time-development operator S_K which is equal to the identity transformation $S_K = I$. Although both selections are completely equivalent, in the following we adopt the former, so that the previous equations are written in the form

$$\frac{\partial w_n}{\partial t} + [w_n, H_0] = \sum_{\mathbf{m}\neq 0} P_{n,\mathbf{m}}(\mathbf{J}, t)\, \mathrm{e}^{\mathrm{i}\mathbf{m}\cdot\theta} \tag{14}$$

and their solutions in the time interval $[t_k, t_{k+1}]$ are given as

$$w_n = \sum_{m\neq 0} F_{n,\mathbf{m}}\, \mathrm{e}^{\mathrm{i}\mathbf{m}\cdot\theta} \tag{15}$$

$$F_{n,\mathbf{m}} = \int_{t_0}^{t} P_{n,\mathbf{m}}(\mathbf{J}, s)\, \mathrm{e}^{\mathrm{i}\mathbf{m}\cdot\omega_{\mathbf{0}}(\mathbf{J})(s-t)}\, \mathrm{d}s \tag{16}$$

with $\omega_{\mathbf{0}}(\mathbf{J}) = \partial H_0/\partial \mathbf{J} = (\partial H_0/\partial J_1, \ldots, \partial H_0/\partial J_N)$ and $t_0 \in [t_k, t_{k+1}]$. Following Deprit [28], the Lie generator w can be obtained to any order with a well-defined procedure. In fact, any calculations in the context of the canonical perturbation theory to higher than second order can be performed practically only by utilizing Lie series; even when mixed-variable generating functions are considered, their derivation utilizes their equivalence with Lie-generating functions w_n, as shown in [30]. For illustrative purposes, in the rest of this work we consider results of the perturbation theory up to second order, so that the expressions are kept rather simple and the properties of the relative transformations are quite clear. Therefore we obtain

$$K_1 = 0 \tag{17}$$

$$F_{1,m} = -\int_{t_0}^{t} H_{\mathbf{m}}(J, s)\, \mathrm{e}^{\mathrm{i}\mathbf{m}\cdot\omega_{\mathbf{0}}(\mathbf{J})(s-t)}\, \mathrm{d}s \tag{18}$$

and

$$K_2 = \frac{\mathrm{i}}{2} \sum_{\mathbf{m}\neq 0} \mathbf{m} \cdot \frac{\partial}{\partial \mathbf{J}} (F_{1,\mathbf{m}} H_{-\mathbf{m}}) \tag{19}$$

$$F_{2,\mathbf{m}} = -\mathrm{i} \sum_{\mathbf{l}} \int_{t_0}^{t} \left(\mathbf{l} \cdot \frac{\partial H_{\mathbf{m}-\mathbf{l}}}{\partial \mathbf{J}} F_{1,\mathbf{l}} - (\mathbf{m} - \mathbf{l}) \cdot \frac{\partial F_{1,\mathbf{l}}}{\partial \mathbf{J}} H_{\mathbf{m}-\mathbf{l}} \right) \mathrm{e}^{\mathrm{i}\mathbf{m}\cdot\omega_{\mathbf{0}}(\mathbf{J})(s-t)}\, \mathrm{d}s \tag{20}$$

The Lie generating function up to second order is then given from equations (15), (18) and (20) and the corresponding mapping is derived directly from equation (7).

It is necessary to emphasize that although the mapping given in equation (7) is symplectic (since the Lie transforms are canonical), the mapping resulting from the truncation of the series expansion at any order is not exactly symplectic. However, the truncated series are converging to the exact Lie transformation, in the limit $\epsilon \to 0$. Thus, for small perturbation parameters where the system (1) is considered as near-integrable, the corresponding mappings can be considered as near-symplectic. The order of the non-symplectic part of these transformations is the same as the order of the corresponding series. Moreover, as we show in the following, the actual series expansion parameter for a finite time interval is the effective perturbation strength ϵ',

$$\epsilon' \sim \epsilon (t - t_0)^{\nu} a(\mathbf{J}), \tag{21}$$

where ν depends on the specific form of the perturbation terms and $a(\mathbf{J})$ is a function of the actions which is localized around the action values corresponding to resonances, similar to the case where mixed-variable generating functions and implicit mappings are considered [23]. This fact allows for the consideration of higher perturbations ϵ, by keeping the time interval $\tau = t_{k+1} - t_k$ small. As will be shown in the next section, the capability of choosing τ small enough in order to provide a high accuracy as well as some non-sympletic behavior, along with the explicit form of the mapping, results in advantageous calculations with respect to implicit mappings utilizing mixed-variable generating functions. It is also worth mentioning that, due to the strong dependence of ϵ' on the actions and its rapid decreasing as the actions move away from their resonant values, it is possible to use larger time steps τ for nonresonant initial conditions.

An interesting case occurring quite commonly in applications is when the perturbation part of the Hamiltonian (1) is time periodic. In such cases, we have

$$H_{\mathbf{m}}(\mathbf{J}, t) = A_{\mathbf{m}}(\mathbf{J})\, \mathrm{e}^{\mathrm{i}\omega_{\mathbf{m}} t} \tag{22}$$

with $A_{-\mathbf{m}} = A_{\mathbf{m}}^*$ and $\omega_{-\mathbf{m}} = -\omega_{\mathbf{m}}$.

For the first-order generating function we obtain

$$F_{1,\mathbf{m}} = -A_{\mathbf{m}}(\mathbf{J})\, \mathrm{e}^{-\mathrm{i}\mathbf{m}\cdot\omega_{\mathbf{0}} t} b_{\Omega_{\mathbf{m}}}(t, t_0) \tag{23}$$

$$b_{\Omega_{\mathbf{m}}}(t, t_0) = \int_{t_0}^{t} \mathrm{e}^{\mathrm{i}\Omega_{\mathbf{m}} s}\, \mathrm{d}s = \frac{\mathrm{e}^{\mathrm{i}\Omega_{\mathbf{m}} t} - \mathrm{e}^{\mathrm{i}\Omega_{\mathbf{m}} t_0}}{\mathrm{i}\Omega_{\mathbf{m}}} \tag{24}$$

where $\Omega_{\mathbf{m}} = \omega_{\mathbf{m}} + \mathbf{m}\cdot\omega_{\mathbf{0}}$. The condition $\Omega_{\mathbf{m}}(\mathbf{J}) = 0$ corresponds to a resonance between the N degrees of freedom and the periodic time forcing. The functions $b_{\Omega_{\mathbf{m}}}$ are strongly localized around the resonances $\Omega_{\mathbf{m}}$, where

$$b_{\Omega_{\mathbf{m}}}(t, t_0)|_{\Omega_{\mathbf{m}}=0} = t - t_0 \tag{25}$$

and their width decreases rapidly with increasing $\Delta t = t - t_0$, having the following limit,

$$\lim_{t\to\infty} b_{\Omega_{\mathbf{m}}}(t, -t) = 2\pi\delta(\Omega_{\mathbf{m}}) \tag{26}$$

with $\delta(\Omega_{\mathbf{m}})$ being Dirac's generalized function.

The second-order term of the new Hamiltonian K_2 and the Lie generator (through (15)) are given as

$$K_2 = -\frac{\mathrm{i}}{2}\sum_{\mathbf{m}\neq 0} \mathbf{m}\cdot\left[\frac{\partial(|A_{\mathbf{m}}|^2 \mathrm{e}^{-\mathrm{i}\Omega_{\mathbf{m}} t})}{\partial \mathbf{J}} b_{\Omega_{\mathbf{m}}}(t, t_0) + \mathrm{i}\frac{\partial\,(\mathbf{m}\cdot\omega_{\mathbf{0}})}{\partial \mathbf{J}} |A_{\mathbf{m}}|^2 \mathrm{e}^{-\mathrm{i}\Omega_{\mathbf{m}} t}\, \mathrm{d}_{\Omega_{\mathbf{m}}}(t, t_0)\right] \tag{27}$$

and

$$F_{2,\mathbf{m}} = -\mathrm{i} \sum_{\mathbf{m_1}+\mathbf{m_2}=\mathbf{m}} \mathrm{e}^{-\mathrm{i}\mathbf{m}\cdot\omega_0 t} \left[\left(-A_{m_1}\mathbf{m_1} \cdot \frac{\partial A_{\mathbf{m_2}}}{\partial \mathbf{J}} + A_{m_2}\mathbf{m_2} \cdot \frac{\partial A_{\mathbf{m_1}}}{\partial \mathbf{J}} \right) \frac{b_{\Omega_{\mathbf{m_1}}+\Omega_{\mathbf{m_2}}} - \mathrm{e}^{-\mathrm{i}\Omega_{\mathbf{m_1}} t_0} b_{\Omega_{\mathbf{m_2}}}}{\mathrm{i}\Omega_{\mathbf{m_1}}} \right.$$

$$\left. -\mathrm{i}A_{\mathbf{m_1}} A_{\mathbf{m_2}} \mathbf{m_2} \cdot \frac{\partial(\mathbf{m_1}\cdot\omega_\mathbf{0})}{\partial \mathbf{J}} \frac{\mathrm{e}^{\mathrm{i}\Omega_{\mathbf{m_1}} t} \left(\mathrm{i}\Omega_{\mathbf{m_2}}\right) \mathrm{d}_{\Omega_{\mathbf{m_2}}} + \mathrm{e}^{\mathrm{i}\Omega_{\mathbf{m_2}} t_0} \left(\mathrm{i}\Omega_{\mathbf{m_1}}\right) \mathrm{d}_{\Omega_{\mathbf{m_1}}} - \mathrm{i}(\Omega_{\mathbf{m_1}} + \Omega_{\mathbf{m_2}}) \mathrm{d}_{\Omega_{\mathbf{m_1}}+\Omega_{\mathbf{m_2}}}}{\left(\mathrm{i}\Omega_{\mathbf{m_1}}\right)\left(\mathrm{i}\Omega_{\mathbf{m_2}}\right)} \right] \tag{28}$$

respectively. The functions

$$\mathrm{d}_{\Omega_\mathbf{m}}(t, t_0) = \int_{t_0}^{t} s\, \mathrm{e}^{\mathrm{i}\Omega_\mathbf{m} s}\, \mathrm{d}s = \frac{(\mathrm{i}\Omega_\mathbf{m} t - 1)\, \mathrm{e}^{\mathrm{i}\Omega_\mathbf{m} t} - (\mathrm{i}\Omega_\mathbf{m} t_0 - 1)\, \mathrm{e}^{\mathrm{i}\Omega_\mathbf{m} t_0}}{(\mathrm{i}\Omega_\mathbf{m})^2} \tag{29}$$

are also localized strongly around the resonances $\Omega_\mathbf{m}$, where

$$\mathrm{d}_{\Omega_\mathbf{m}}(t, t_0)|_{\Omega_\mathbf{m}=0} = \frac{t^2 - t_0^2}{2} \tag{30}$$

and their width decreases rapidly with increasing $\Delta t = t - t_0$ with the limit

$$\lim_{t\to\infty} \mathrm{d}_{\Omega_\mathbf{m}}(t, -t) = \mathrm{i}2\pi\delta'(\Omega_\mathbf{m}) \tag{31}$$

where $\delta'(\Omega_\mathbf{m})$ is the derivative of Dirac's generalized function.

Note that, similarly to the case of mixed-variable generating functions, the consideration of finite time intervals prevents the appearance of the well-known problem of small denominators [23].

3. Accuracy and comparison with implicit symplectic mappings

In the following, we study the accuracy of the explicit mapping obtained in the previous section, with the implicit symplectic mapping obtained with the utilization of mixed-variable generating functions [23]. As an example we use the Hamiltonian system

$$H = \frac{J^2}{2} - \left(\epsilon \frac{J}{2} \mathrm{e}^{\mathrm{i}(m\theta - \omega_m t)} + \mathrm{c.c.} \right) \tag{32}$$

which is integrable with

$$H' = \frac{J^2}{2} - \frac{\omega_m}{m} J - \epsilon J \cos(m\theta - \omega_m t) \tag{33}$$

being a constant of the motion. The preservation of this constant under successive mapping iterations is used as a measure for the comparison of the accuracy of the mappings. Note that the system (32) is not separable, so that there are no explicit exact symplectic mappings, since the method of [26] is not applicable. Moreover, the system used as an example has been chosen so that the unperturbed Hamiltonian $H_0 = J^2/2$ corresponds to a nonlinear system for which the unperturbed frequencies are functions of the action $\mathrm{d}\omega_0/\mathrm{d}J = \mathrm{d}^2 H_0/\mathrm{d}J^2 \neq 0$. In this general case, the resonance conditions are met only locally in the phase space, in contrast to the case of unperturbed linear systems where the resonant conditions are satisfied either in the entire phase space or nowhere. The latter case is characterized as degenerate, and is a well-known situation where the application of the KAM theory fails (the condition of sufficient nonlinearity is not satisfied [2]). To our knowledge, explicit mappings utilizing Lie-generating functions have been compared to implicit mappings, only for such a degenerate case [20], where it is shown that for the nonresonant case ([20], chapter 4) the deviation from the actual solution is periodic in time for the implicit mappings and continiously increasing

for the explicit one. For the resonant case ([20], chapter 2) both methods provide results with increasing deviation from the actual solution as time increases, with the implicit method deviating at much longer times than the explicit ones. The reason for this behavior is that when the resonant condition is met, the functions $a(J)$ related to the effective perturbation strength (21) (or $b_{\Omega_m}(t, t_0)$ for the first-order generating functions in the periodic case) attain their extreme value in every time step, since the resonant condition is fulfilled for every action value, resulting in higher effective perturbation strength and higher error in each step, which accumulates continuously. However, in the following it is shown that the situation for the general nondegenerate case of a nonlinear unperturbed system, such as (32), is completely different.

According to [23], the implicit mapping has the following form,

$$J'(t_k) = J(t_k) - \frac{\partial S(J'(t_k), \theta(t_k), t_k)}{\partial \theta}$$
$$\theta'(t_k) = \theta(t_k) + \frac{\partial S(J'(t_k), \theta(t_k), t_k)}{\partial J'} \tag{34}$$

$$J'(t_{k+1}) = J'(t_k)$$
$$\theta'(t_{k+1}) = \theta'(t_k) + \int_{t_k}^{t_{k+1}} \frac{\partial K(J', s)}{\partial J'}\, \mathrm{d}s \tag{35}$$

$$J(t_{k+1}) = J'(t_{k+1}) + \frac{\partial S(J'(t_{k+1}), \theta(t_{k+1}), t_{k+1})}{\partial \theta}$$
$$\theta(t_{k+1}) = \theta'(t_{k+1}) - \frac{\partial S(J'(t_{k+1}), \theta(t_{k+1}), t_{k+1})}{\partial J'}, \tag{36}$$

where S is the mixed-variable generating function. This mapping is the implicit analogue of the explicit mapping (7) with (34) and (36) corresponding to T and T^{-1}, respectively, and (35) being $S_K(t_{k+1}, t_k)$. It is worth mentioning that the Lie-generating functions w are related to the mixed-variable generating functions S at every order with respect to the perturbation parameter ϵ [30] and particularly for the first order

$$S_1(J', \theta, t) = w_1(J = J', \theta, t) \tag{37}$$

From the computational point of view the implicit form of the mapping necessitates the utilization of a numerical method for solving the corresponding algebraic equations. In the following we have used the well-known Newton–Raphson method which has a quite high rate of convergence. At each step of the mapping we use as an initial value of the Newton–Raphson iterative procedure $J(t_k)$ in the first equation of (34) and $\theta'(t_{k+1})$ in the second equation of (36), since the differences of these initial values with the actual values are of the order of the effective perturbation strength ϵ' (21). Therefore, each time step of the implicit mapping includes a number of internal steps for two Newton–Raphson procedures required for the solution of the corresponding algebraic equations. As we show in the following, for the same size of time step τ, the implicit mapping, although more accurate in most cases, is much more time consuming than the explicit mapping of the same order. The advantage of the speed of the explicit map, in comparison to the implicit one is expected to be even more significant for systems with large number of degrees of freedom, where the internal steps required for the solution of the implicit algebraic equations involve calculation and inversion of Jacobians which is quite time-consuming. Also, the speed difference is expected to increase for higher order mappings where the corresponding algebraic equations are more complex and the respective evaluations in the Newton–Raphson procedure are more time consuming.

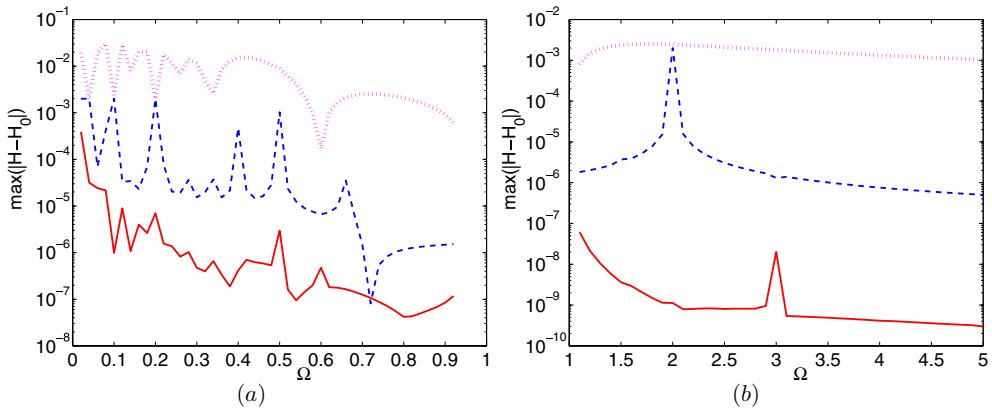

Figure 1. Maximum error in the calculation of the Hamiltonian $\max(|H - H_0|)$ versus external frequency Ω for perturbation strength $\epsilon = 10^{-3}$, initial conditions $(J_0, \theta_0) = (1, 0)$, time step $\tau = 2\pi/\Omega$ and total time 1000τ. Dotted (magenta) and solid (red) curves correspond to first- and second-order explicit maps, respectively; dashed (blue) curves correspond to first-order implicit map.

Without loss of generality, we consider the system (32) with $m = 1, \omega_m = \Omega$. Since the system is integrable, the phase portrait of the system in the Poincaré surface of section for $t_i = \mathrm{i}2\pi/\Omega, i = 1, 2, \ldots$, can be obtained from the constant of the motion (33). The Poincaré surfaces of section consist of two distinct areas distinguished by a separatrix. The inner area is located around the resonant action value and characterized by an angle trapping (libration type of oscillations), while in the area outside the separatrix the phase runs in the entire interval $[0, 2\pi]$ (rotation type of oscillation). The width of the resonant area, measured at the separatrix, increases with the perturbation strength ϵ. Note that in the generic case of a Hamiltonian system with many periodic perturbative terms of the form (22), the Poincaré surfaces of section consist of many resonant areas, which appear chaotic near their separatrices, while extended chaotic areas appear when the resonances overlap [2].

We consider the case of a perturbation $\epsilon = 10^{-3}$ and study explicit and implicit mappings with the choice of the free parameter $t_0 \in [t_k, t_{k+1}]$ so that $t_0 = t_k + \tau/2$, corresponding to the symmetric mapping [23]. Note that the results can be applied directly for cases of higher perturbations ϵ, by simply reducing the time step τ so that the effective perturbation strength ϵ' (21) is kept small. Below we use the conserved quantity as a measure of the accuracy of the mappings by considering the quantity $\Delta H'(t) = |H'(t) - H'(0)|$. Firstly, we investigate the dependence of the accuracy on the external frequency Ω for a fixed initial condition $(J_0, \theta_0) = (1, 0)$. Since the internal frequency (for $\epsilon = 0$) is $\omega = \partial H_0/\partial J = J$, the initial condition corresponds to $\omega = 1$. In figures 1(*a*) and (*b*) the maximum error in the conservation of the Hamiltonian is depicted for $\Omega < \omega$ and $\Omega > \omega$, respectively, for the first-order implicit map as well as for the first- and second-order explicit maps. It is shown that the first-order implicit map is more accurate than the first-order explicit map, but less accurate than the second-order explicit map. Moreover, for the implicit map the accuracy is shown to deteriorate for several values of Ω corresponding to resonances between the internal and the external frequencies $m_1\omega = m_2\Omega$. A similar behavior is also observed in the study of the accuracy as a function of the initial condition $(J_0, 0)$ for a fixed external frequency Ω, as shown in figures 2(*a*) and (*b*). It is important to emphasize the significance of the behavior of the mappings for different initial conditions: for a nondegenerate (nonlinear) system the

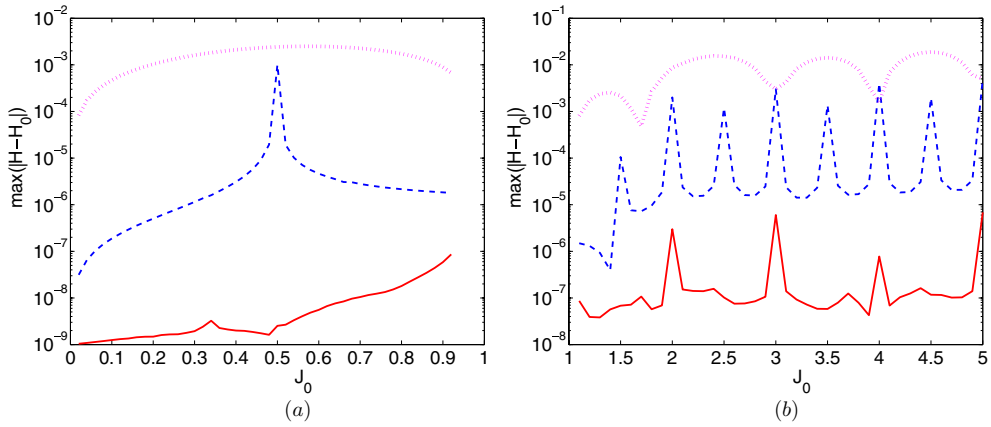

Figure 2. Maximum error in the calculation of the Hamiltonian $\max(|H - H_0|)$ versus initial condition J_0 for perturbation strength $\epsilon = 10^{-3}$, external frequency $\Omega = 1$, initial conditions $(J_0, \theta_0) = (J_0, 0)$, time step $\tau = 2\pi/\Omega$ and total time 1000τ. Dotted (magenta) and solid (red) curves correspond to first- and second-order explicit maps, respectively; dashed (blue) curves correspond to first-order implicit map.

internal frequency is a function of the action, so that we can have a wide range of internal frequencies in the phase space. It is worth mentioning that the behavior and accuracy of the implicit symmetric map, for a system such as the one under consideration, have been studied only near the resonances and for a libration type of motion. As can be seen in [23, 20] the initial actions and the external frequencies are chosen so that $(J - \Omega)/J_{\text{separatrix}}$ is within the interval [0, 1]. This is a very restricted area of the phase (or parameter) space, especially for small perturbations (of the order interesting for applications), where the external frequency is very close to the frequency of the internal degree of freedom. However, the cases of larger differences between the internal and the external frequencies have not been investigated so far.

As shown in figure 2 there are specific peaks in the error in the preservation of the Hamiltonian for the implicit mapping corresponding to resonances, appearing for initial conditions far from the $\Omega = \omega = J$. The latter are related not only to quantitative inaccuracy but also to qualitatively (topologically) different Poincaré surfaces of section. Specific examples of such cases are depicted in figures 3(*a*) and (*b*) for $J_0 = \Omega/2$ and $J_0 = 2\Omega$, respectively. For these cases, the first-order implicit map introduces spurious phase-space islands in the Poincaré surfaces of section. On the other hand, the first-order explicit map results in an inaccurate results since the corresponding curves are not closed so that artificial dissipation is introduced and the phase-space orbits are not periodic. However, the second-order explicit map results in accurate construction of the Poincaré surface of section. All previous results have been utilizing maps with a step corresponding to a period of the driving force $\tau = 2\pi/\Omega$ as needed for the (stroboscopic) construction of the Poincaré surface of section. For all maps, the accuracy can be further improved by using N steps of calculation within an external period, resulting in a time step $\tau = 2\pi/\Omega N$. As the time step decreases, the accuracy is improved, and the spurious orbits in the Poincaré surfaces of section disappear, while the calculation time t_{rcpu} is also increased. In figures 4(*a*) and (*b*) the accuracy of the mappings as a function of the corresponding t_{rcpu} is presented for the cases where $N = 1, \ldots, 10$ steps of calculation within an external period are used, and for initial conditions corresponding to figures 3(*a*) and (*b*), respectively. It is shown that for small

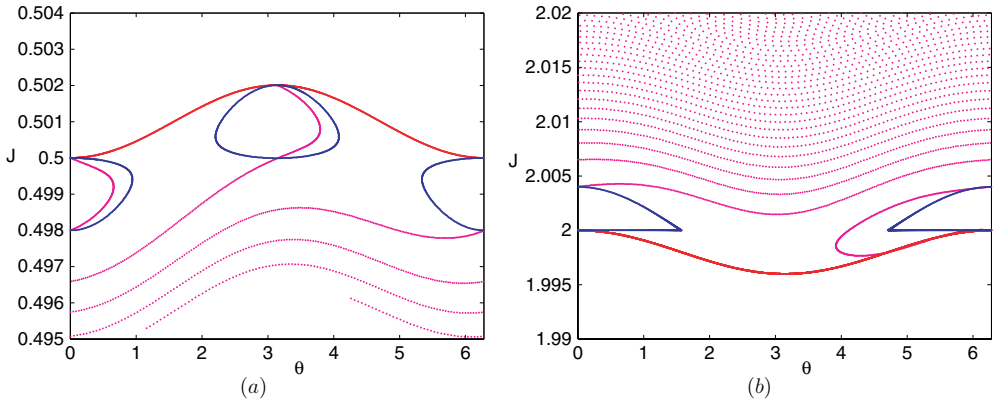

Figure 3. Poincaré surfaces of section for initial conditions $(J_0, \theta_0) = (1/2, 0)$ (a) and $(J_0, \theta_0) = (2, 0)$ (b), perturbation strength $\epsilon = 10^{-3}$, external frequency $\Omega = 1$, time step $\tau = 2\pi/\Omega$ and total time 1000τ. Magenta and red curves correspond to first- and second-order explicit maps, respectively; blue curves correspond to first-order implicit map.

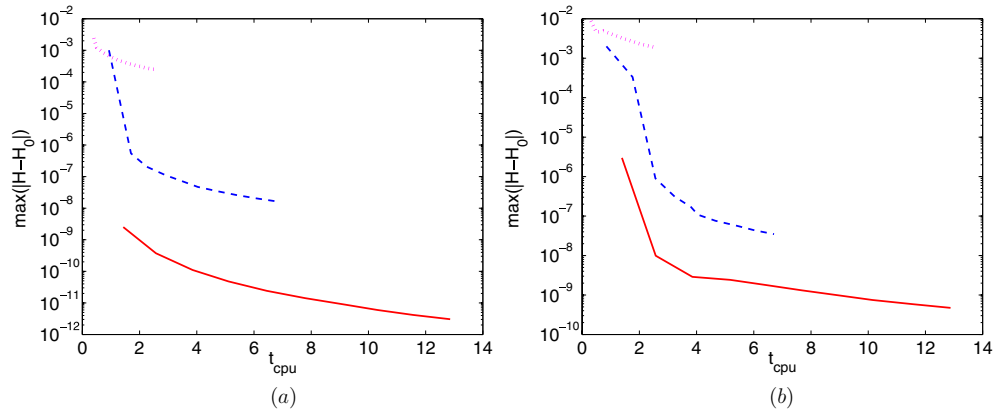

Figure 4. Maximum error in the calculation of the Hamiltonian $\max(|H - H_0|)$ versus calculation (cpu) time t_{rcpu} for initial conditions $(J_0, \theta_0) = (1/2, 0)$ (a) and $(J_0, \theta_0) = (2, 0)$ (b), perturbation strength $\epsilon = 10^{-3}$, external frequency $\Omega = 1$, time step $\tau = 2\pi/\Omega N$, $(N = 1, \ldots, 10)$ and total time 1000τ. Dotted (magenta) and solid (red) curves correspond to first- and second-order explicit maps, respectively; dashed (blue) curves correspond to first-order implicit map.

N (small t_{rcpu}) the accuracies of the first order implicit and explicit maps are comparable. The error of the first-order implicit map decreases for an increasing N with the rapid change around $t_{cpu} = 2$ related to the disappearance of the spurious islands. It is remarkable that the second-order explicit map provides better accuracy than the first-order implicit map for the same calculation time t_{rcpu}. The latter is a generic characteristic that is met not only for these specific initial conditions for which the peaks in error apear in figure 2. As shown in figures 5(a) and (b), this is also the case for most initial conditions e.g. $J_0 = 2.3$ and $J_0 = 0.4$. Moreover, the advantage of the second-order implicit map in terms of accuracy and calculation time persists for cases of stronger or weaker perturbations as shown in figures 5(c), (d), (e) and (f) respectively. The explicit form of the second-order mapping, utilizing Lie-generating

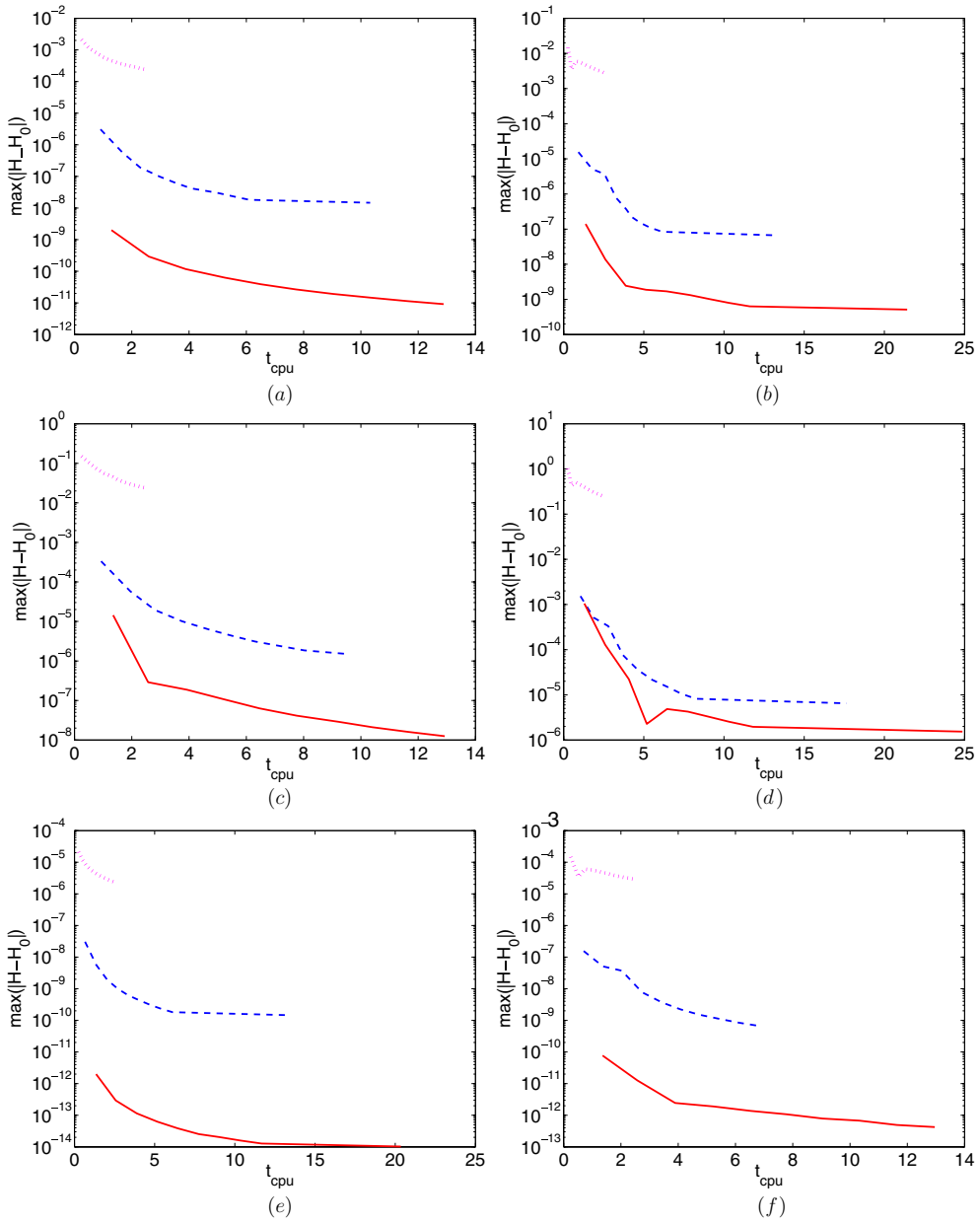

Figure 5. Maximum error in the calculation of the Hamiltonian $\max(|H - H_0|)$ versus calculation (cpu) time t_{rcpu} for initial conditions $(J_0, \theta_0) = (0.4, 0)$ (a), (c), (e) and $(J_0, \theta_0) = (2.3, 0)$ (b), (d), (f), perturbation strength $\epsilon = 10^{-3}$ (a), (b), $\epsilon = 10^{-2}$ (c), (d), $\epsilon = 10^{-4}$ (e, f), external frequency $\Omega = 1$, time step $\tau = 2\pi/\Omega N$, $(N = 1, \ldots, 10)$ and total time 1000τ. Dotted (magenta) and solid (red) curves correspond to first- and second-order explicit maps, respectively; dashed (blue) curves correspond to first-order implicit map.

functions, results in more accurate calculations in comparison to a first-order implicit mapping, utilizing mixed-variable generating functions, for a fixed calculation time. This is due to the fact that the calculation speed of the explicit map allows for the utilization of a smaller time

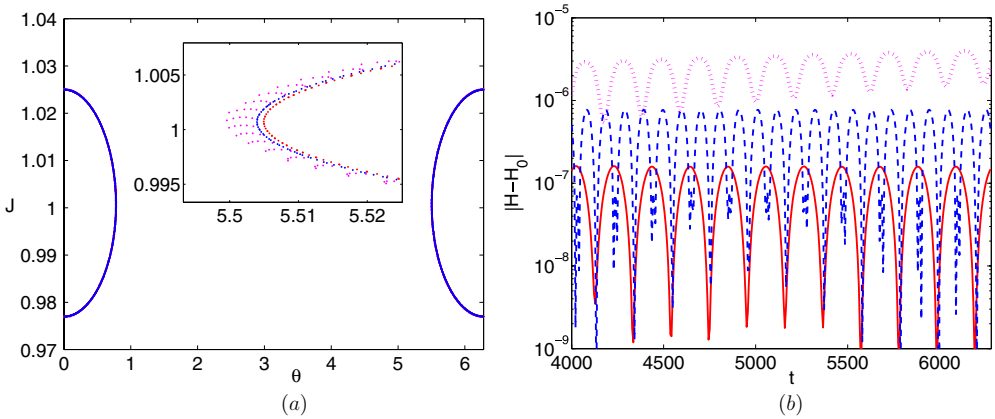

Figure 6. (*a*) Poincaré surface of section and (*b*) error in the calculation of the Hamiltonian $|H - H_0|$ versus time t, for initial conditions $(J_0, \theta_0) = (1.025, 0)$ corresponding to libration type of motion, perturbation strength $\epsilon = 10^{-3}$, external frequency $\Omega = 1$, time step $\tau = 2\pi/\Omega$, and total time 1000τ. Dotted (magenta) and solid (red) curves correspond to first- and second-order explicit maps, respectively; dashed (blue) curves correspond to first-order implicit map.

step (larger N) than that utilized for the implicit map, while keeping the same calculation (cpu) time same. The efficiency of the second-order explicit map suggests that such a map is useful for applications where time-consuming calculations are involved and accuracy is important. Depending on the perturbation strength ϵ and the desired accuracy, there are many practical cases where the second-order explicit map is the most appropriate calculation scheme, while for very small perturbation strength $\epsilon < 10^{-4}$ even the first-order explicit map is capable of providing accurate results.

Finally, we complete the comparison between the aforementioned mappings for the case of initial conditions located within the area inside the separatrix of the resonance $\omega = \Omega$ and corresponding to a libration type of motion. In figures 6(*a*) and (*b*) the Poincaré surface of section and the error in the Hamiltonian as a function of time, respectively, are depicted for the case of a perturbation strength $\epsilon = 10^{-3}$ and initial condition $(J_0, \theta_0) = (1.025, 0)$. The accuracies of the three mappings follow the same ordering as with the previous cases, while their differences are smaller.

4. Conclusions

In this work, we consider the construction of explicit near-symplectic mappings, with the utilization of the Lie transform perturbation theory in finite time intervals. These mappings although not exactly symplectic, due to the truncation of the corresponding series, are shown to have a remarkable accuracy and capability of conserving the invariants of the motion, while being very fast in terms of calculation (CPU) time.

The explicit maps are studied in comparison to implicit ones utilizing mixed-variable generating functions, for a specific Hamiltonian system and a variety of parameters and initial conditions. Particular emphasis is given to the cases where there exist large differences between characteristic frequencies of the system, since for a nondegenerate (nonlinear) system, where the internal frequencies are functions of the actions, different initial conditions in the phase space are related to a wide range of frequencies. The efficiencies of the explicit and implicit

mappings are discussed in terms of their accuracy with respect to conservation of certain invariants of the motion. It is shown that the first-order implicit map is more accurate than the explicit map of the same order but less accurate than the second-order explicit map, for a fixed time step. However, the fact that explicit maps are much faster than the implicit ones allows us to reduce the time step for the explicit maps so that for the same calculation (cpu) time, a second-order explicit map provides better accuracy than a first-order implicit map. It is also shown that for quite small perturbation strengths, even a first-order explicit map provides quite accurate results in a very short calculation time. It is expected that application of the discussed explicit mappings will be proved as a useful tool for the study of a great variety of problems in many areas of physics.

Acknowledgments

This work was supported in part by the European Fusion Programme (EURATOM), the Greek General Secretariat of Research and Technology and the Romanian Ministry of Education and Research.

References

[1] Meiss J D 1992 Symplectic maps, variational principles and transport *Rev. Mod. Phys.* **64** 795
[2] Lichtenberg A J and Lieberman M A 1992 *Regular and Chaotic Dynamics* (New York: Springer)
[3] Goldstein H 1980 *Classical Mechanics* (Reading, MA: Addison-Wesley)
[4] Arnold V I 1979 *Mathematical Methods of Classical Mechanics* (New York: Springer)
[5] Boozer A H 1983 Evaluation of the structure of ergodic fields *Phys. Fluids* **26** 1288
[6] Balescu R, Vlad M and Spineanu F 1998 Tokamap: a Hamiltonian twist map for magnetic field lines in toroidal geometry *Phys. Rev.* E **58** 951
[7] Pavlenko I, Rapoport B, Weyssow B and Carati D 2003 Hamiltonian mapping of magnetic reconnection during the crash stage of the sawtooth instability *Phys. Plasmas* **10** 1083
[8] Abdullaev S S 2004 On mapping models of field lines in a stochastic magnetic field *Nucl. Fusion* **44** S12
[9] Boozer A H 2004 Physics of magnetically confined plasmas *Rev. Mod. Phys.* **76** 1071
[10] Dumbrajs O, Igochine V, Constantinescu D and Zohm H 2005 Stochastization as a possible cause of fast reconnection in the frequently interrupted regime of neoclassical tearing modes *Phys. Plasmas* **12** 110704
[11] Igochine V, Dumbrajs O, Constantinescu D, Zohm H and Zvejnieks G 2006 Stochastization as a possible cause for fast reconnection during MHD mode activity in the ASDEX upgrade tokamak *Nucl. Fusion* **46** 741
[12] Abdullaev S S, Finken K H and Spatschek K H 1999 Asymptotical and mapping methods in study of ergodic divertor magnetic field in a toroidal system *Phys. Plasmas* **6** 153
[13] Abdullaev S S, Finken K H, Jakubowski M and Lehnen M 2006 Mappings of stochastic field lines in poloidal divertor tokamaks *Nucl. Fusion* **46** S113
[14] Kominis Y, Dumbrajs O, Avramides K A, Hizanidis K and Vomvoridis J L 2005 Canonical perturbation theory for complex electron dynamics in gyrotron resonators *Phys. Plasmas* **12** 113102
[15] Kominis Y, Hizanidis K and Ram A K 2006 Transient dynamics of charged particles interacting with localized waves of continuous spectra *Phys. Rev. Lett.* **96** 025002
[16] Dumbrajs O, Kominis Y, Avramides K A, Hizanidis K and Vomvoridis J L 2006 Hamiltonian map description of electron dynamics in gyrotrons *IEEE Trans. Plasma Sci.* **34** 673
[17] Dragt A J and Forest E 1983 Computation of nonlinear behavior of Hamiltonian systems using Lie algebraic methods *J. Math. Phys.* **24** 2734
[18] Dragt A J 1982 Lie algebraic theory of geometrical optics and optical aberrations *J. Opt. Soc. Am.* **72** 372
[19] Dragt A J 1995 Computation of maps for particle and light optics by scaling, splitting and squaring *Phys. Rev. Lett.* **75** 1946
[20] Abdullaev S S 2006 *Construction of Mappings for Hamiltonian Systems and Their Applications (Lect. Notes Phys.* vol 691) (Berlin, Heidelberg: Springer)
[21] Forest E 2006 Geometric integration for particle accelarators *J. Phys. A: Math. Gen.* **39** 5321
[22] Chirikov B V 1979 A universal instability of many-dimensional oscillator systems *Phys. Rep.* **52** 263
[23] Abdullaev S S 2002 The Hamilton–Jacobi method and Hamiltonian maps *J. Phys. A: Math. Gen.* **35** 2811

[24] Ruth R D 1983 A canonical integration technique *IEEE Trans. Nucl. Sci.* **30** 2669
[25] Yoshida H 1990 Construction of higher order symplectic integrators *Phys. Lett.* A **150** 262
[26] McLachlan R I and Atela P 1992 The accuracy of symplectic integrators *Nonlinearity* **5** 541
[27] Cary J R 1981 Lie transform perturbation theory for Hamiltonian systems *Phys. Rep.* **79** 129
[28] Deprit A 1969 Canonical transformations depending on a small parameter *Celest. Mech.* **1** 12
[29] Dragt A J and Finn J M 1976 Lie series and invariant functions for analytic symplectic maps *J. Math. Phys.* **17** 2215
[30] Shniad H 1970 The equivalence of Von Zeipel mappings and Lie transforms *Celest. Mech.* **2** 114